

Validation of the continuum orthotropic model of tensegrity beam-like and plate-like structures

P. OBARA, J. TOMASIK

Department of Civil Engineering, Kielce University of Technology, Kielce, Tysiąclecia Państwa Polskiego 7, 25-314 Kielce, Poland, e-mail: jtomasik@tu.kielce.pl

IN THIS PAPER, AN ATTEMPT WAS MADE TO DEVELOP THE CONTINUUM ORTHOTROPIC MODEL of tensegrity structures. A basic four-module tensegrity grid built from modified Quadruplex modules was proposed. A procedure called the energy equivalency method was adopted. The basis of this approach is the assumption that the finite element strain energy of a deformed tensegrity truss system contains the same energy as its continuum counterpart. Next, the six-parameter shell theory was used and closed forms for maximum displacements were obtained. Finally, in order to fill the gap in the existing literature, the continuum model was validated – the displacements were compared with displacements obtained from a discrete nonlinear model (the finite element method). The continuum model of tensegrity is a simple tool for analyzing large beam-like structures, plate-like structures and plate strips. It is important in case when discrete modeling becomes too tedious for the analysis. Another point is that many commercial software programs cannot analyze structures characterized by mechanisms. The finding of this work can also be useful for modeling metamaterials whose topology is based on the concept of tensegrity.

Key words: tensegrity, double-layered grid, self-stress, infinitesimal mechanism, continuum orthotropic model, discrete model.



Copyright © 2023 The Authors.

Published by IPPT PAN. This is an open access article under the Creative Commons Attribution License CC BY 4.0 (<https://creativecommons.org/licenses/by/4.0/>).

1. Introduction

ONE OF THE WIDELY INVESTIGATED APPLICATIONS OF TENSEGRITY STRUCTURES are double-layer tensegrity grids [1–3]. The rigidity and stability of these reticulate strut-and-cable systems are conditioned by the existence of self-stress states. A self-stress state is a self-equilibrium system of internal forces, which stabilizes existing infinitesimal mechanisms. The specificity of tensegrity grids is repeatability. The elements are arranged in a regular pattern and organized into two parallel planes forming upper and lower layers. Due to their similarity to traditional structural systems, the grids are called tensegrity beam-like or plate-like structures. These structures can be built from the base tensegrity modules, such as Quadruplex [4–6].

Double-layer tensegrity grids can be analyzed using a discrete model, i.e. the finite element method (FEM), or a continuum model. The first approach is the most popular [1–6]. However, in the case of large FEM structures, it requires significant computing power. In addition, popular structural analysis programs do not allow for the analysis of structures characterized by mechanisms. Hence, equivalent continuum modeling techniques have promising advantages. By reducing the degrees of freedom, the continuum model is a practical and efficient approach for analyzing large grids. This approach also provides an easy way to compare characteristics of structures with different configurations and assesses their response to changes in material and geometric properties. Moreover, continuum modeling is an effective tool for designing control systems of tensegrity grids. This is because in such situations only the global behavior of the structure is of interest, and detailed information of each element is not needed. The number of publications on continuum modeling of repetitive lattice structures is steadily increasing. The state of research about the equivalent continuum modeling of these structures is presented by LIU *et al.* [7]. The authors described advantages and future directions of this approach. Applications of the continuum model to some beam-like and plate-like tensegrity lattices have been proposed, among others, by NOOR and MIKULAS [8], NOOR [9], TEUGHELIS [10] and NEMETH [11]. In the case of tensegrity trusses, the continuum model was used in [12–16]. KEBICHE *et al.* [12] presented a procedure for determining the equivalent continuum properties of systems characterized by self-stress states. This procedure was based on the energy equivalence between the discrete model and the continuum model. The equivalent continuum properties of tensegrity structures were determined after four matrix transformations based on the approach proposed by DOW *et al.* [17]. The proposed approach was validated on three basic types of tensegrity modules. The equivalent rigidities and coupling terms obtained on these modules were presented and compared with those obtained by the finite element method. Particularly, the influence of the initial prestress on the equivalent stiffness was investigated. YILDIZ and LESIEUTRE [13] also used the energy equivalency method to build continuum beam-like counterparts of tensegrity towers. The obtained equivalent stiffness properties were validated by nonlinear finite element analyses. Moreover, the continuum model of the tensegrity structures were studied by the team of SABOUNI-ZAWADZKA [14–16]. In [14, 15], technical coefficients in continuum models of anisotropic tensegrity modules were described. The continuum models of the modules were obtained by the comparison between strain energies [12, 13]. In turn, in [16] the authors propose the use of the linear six-parameter flat shell theory [18–23] to obtain the continuum model of orthotropic tensegrity plate-like structures, taking into account self-stress states. Tensegrity modules, based on the shape of four-strut expanded octahedron mod-

ules with additional connecting cables, were analyzed. Closed form solutions for selected tensegrity plate strips and the simply supported rectangular plate with sinusoidal load were presented. Taking into account the shell theory, the middle plane was taken as the reference surface. OBARA [24, 25] also applied the linear six-parameter shell theory to the analysis of orthotropic plate-like tensegrity structures [24] and plate strips [25], but took into account different support planes of a structure and thus different reference surfaces of the plate model.

In the literature known to the authors, there is no validation of the global behavior of beam- and plate-like tensegrity structures modeled using continuum approach and characterized by the existence of mechanisms. In [12, 13], only the coefficients of the stiffness matrix were validated. Therefore, this paper develops the prior research by authors of this paper [24, 25] and checks the applicability of the continuum approach. To verify the global behavior of tensegrity structures, the authors provide a comparison of the displacements of the structures modeled using discrete and continuum approaches.

A basic orthotropic four-module tensegrity grid built from modified Quadruplex modules was proposed in this paper. This module can be clustered into beam-like or plate-like structures. The considerations covered a comprehensive approach, i.e. qualitative and quantitative assessment. Two models of structures were taken into account, i.e. the continuum model and the discrete model. The procedure led to the determination of the impact of initial prestress on the static behavior of double-layers grids. Firstly, the continuum model was obtained. The derivation of the equivalent continuum properties of the basic orthotropic module was based on the energetic equivalence between the discrete model and the continuum model. Due to the orthotropic properties of the basic module, it was possible to apply the six-parameter shell theory proposed previously by the authors [25, 26] and closed forms for the maximum displacements were obtained. Finally, in order to fill the gap in the existing literature, the continuum model was validated – the displacements were compared with those obtained using the discrete nonlinear model (the finite element method).

2. Method of analysis

Double layered tensegrity grids can be modeled with finite truss elements or, due to their repetitive character, with a two-dimensional continuum model (for plate-like structures) or a one-dimensional continuum model (for beam-like structures). In the first approach (a discrete model), the structure is analyzed by the finite element method, while in the continuum model, it is analyzed using the solid theory. The solid may generally be described by anisotropic characteristics or, in special cases, by simpler orthotropic ones. Regardless of the type of an

adopted model, the qualitative analysis must be carried out. This assessment is required to determine intrinsic features like infinitesimal mechanisms and self-equilibrated systems of longitudinal forces (self-stress states). Only the discrete model can be used to identify the characteristic features of tensegrities.

2.1. Qualitative assessment

The qualitative assessment determines the intrinsic features of tensegrity structures. Both of them depend only on the compatibility matrix [26, 27]. The analysis is provided for a n -element spatial lattice system with m degrees of freedom described by the nodal displacement vector \mathbf{q} ($\in \mathbb{R}^{m \times 1}$). The compatibility matrix \mathbf{B} ($\in \mathbb{R}^{n \times m}$) is determined using the finite element formalism [28, 29]. Zero eigenvalues of the matrix $\mathbf{B}\mathbf{B}^T$ ($\in \mathbb{R}^{n \times n}$) are responsible for the existence of self-stress states, while zero eigenvalues of the matrix $\mathbf{B}^T\mathbf{B}$ ($\in \mathbb{R}^{m \times m}$) correspond to existence of infinitesimal mechanisms. The self-stress state is considered as an eigenvector \mathbf{y}_S related to the zero eigenvalue of the matrix $\mathbf{B}\mathbf{B}^T$. The self-equilibrated systems of longitudinal forces \mathbf{S} depend on the eigenvector \mathbf{y}_S and the initial prestress level ($\mathbf{S} = \mathbf{y}_S S$).

2.2. Quantitative assessment

The qualitative assessment leads to the determination of the impact of initial prestress level S on the displacements \mathbf{q} of the structure under the static external load. The consideration contains the determination of the minimum (S_{\min}) and maximum (S_{\max}) initial prestress level. The lowest level of initial prestress S_{\min} must ensure the appropriate identification of the element type, while maximum S_{\max} should not increase the loads above the limits of the load-bearing elements N_{Rd} . Two models of structures were taken into account, i.e. the continuum model and the discrete model.

2.2.1. Continuum model. The constitutive equation for the linear theory of elasticity is expressed as:

$$(2.1) \quad \boldsymbol{\sigma} = \mathbf{E}\boldsymbol{\varepsilon},$$

where: $\boldsymbol{\sigma}$ ($\in \mathbb{R}^{6 \times 1}$) – the stress vector, $\boldsymbol{\varepsilon}$ ($\in \mathbb{R}^{6 \times 1}$) – the strain vector and \mathbf{E} ($\in \mathbb{R}^{6 \times 6}$) – the matrix of elasticity.

The matrix of elasticity contains 36 components, including 21 independent ones if there is no material symmetry (anisotropic material). The symmetry results in reduction of the number of elastic moduli [31]. There are exactly eight different sets of symmetry planes. One of them is the orthogonal symmetry

(orthotropic material). This material requires 9 elastic constants for a three-dimensional case. The paper discusses orthotropic tensegrity plate-like structures based on the Reissner–Mindlin theory (excluding stress σ_z and strain ε_z ; $\boldsymbol{\sigma}$ ($\in \mathbb{R}^{5 \times 1}$), $\boldsymbol{\varepsilon}$ ($\in \mathbb{R}^{5 \times 1}$)). For this model, the matrix of elasticity \mathbf{E} ($\in \mathbb{R}^{5 \times 5}$) contains 6 nonzero independent components and Eq. (2.1) can be written as:

$$(2.2) \quad \begin{bmatrix} \sigma_x \\ \sigma_y \\ \sigma_{xy} \\ \sigma_{xz} \\ \sigma_{yz} \end{bmatrix} = \begin{bmatrix} d_{11} & d_{12} & 0 & 0 & 0 \\ d_{12} & d_{22} & 0 & 0 & 0 \\ 0 & 0 & d_{44} & 0 & 0 \\ 0 & 0 & 0 & d_{55} & 0 \\ 0 & 0 & 0 & 0 & d_{66} \end{bmatrix} \begin{bmatrix} \varepsilon_x \\ \varepsilon_y \\ \varepsilon_{xy} \\ \varepsilon_{xz} \\ \varepsilon_{yz} \end{bmatrix}.$$

The method of obtaining the equivalent continuum characteristics used in the paper is based on the energy equivalency method. It is assumed that the finite element strain energy of a deformed tensegrity truss system contains the same energy as its continuum counterpart. To take an advantage of energy equality, the nodal displacement vector $\mathbf{q} = \mathbf{q}^{\text{FEM}}$ ($\in \mathbb{R}^{m \times 1}$) must be formulated as a function of the strains of the equivalent continuum solid model. A repetitive, basic orthotropic unit must be isolated from the considered beam-like or plate-like structure. The displacement field of that repetitive unit $\mathbf{q}^{3\text{D}}(x, y, z) = [u, v, w]^T$ can be expressed using complete third order polynomial representations with respect to the local origin of the unit:

$$(2.3) \quad \begin{aligned} u(x, y, z) &= a_1 + a_2x + a_3y + a_4z + \dots + a_{20}xyz, \\ v(x, y, z) &= b_1 + b_2x + b_3y + b_4z + \dots + b_{20}xyz, \\ w(x, y, z) &= c_1 + c_2x + c_3y + c_4z + \dots + c_{20}xyz. \end{aligned}$$

To calculate 60 coefficients a_n, b_n, c_n which appear in (2.3) and express them in terms of strains describing the continuum body, the polynomials of the displacement must be written as the Taylor series expansion, respectively differentiated and evaluated at the origin of the local coordinate system of the repetitive module. The strain vector consists of 60 coefficients $\boldsymbol{\varepsilon}$ ($\in \mathbb{R}^{60 \times 1}$): five resultant fundamental strains $\varepsilon_x, \varepsilon_y, \varepsilon_{xy}, \varepsilon_{xz}, \varepsilon_{yz}$, six rigid body motions $u_0, v_0, w_0, \phi_1, \phi_2, \phi_3$, strain ε_z and forty eight strain gradients $\varepsilon_{x,x}, \dots, \varepsilon_{y,z,z}, \dots, \varepsilon_{x,xx}, \dots, \varepsilon_{yz,zz}$. From this point, four matrix transformations must be applied to determine the elasticity matrix [12].

First transformation – from discrete displacements to continuous strains

The first transformation consists in applying the assumption of energy equivalence of the modeled continuous structure:

$$(2.4) \quad E_s^{3\text{D}} = \frac{1}{2} \boldsymbol{\varepsilon}^T \mathbf{E} \boldsymbol{\varepsilon}$$

and its counterpart in the discrete model:

$$(2.5) \quad E_s^{\text{FEM}} = \frac{1}{2} \mathbf{q}^T \mathbf{K} \mathbf{q},$$

where \mathbf{K} ($\in \mathbb{R}^{m \times m}$) – the stiffness matrix:

$$(2.6) \quad \mathbf{K} = \mathbf{K}_L + \mathbf{K}_G(\mathbf{S})$$

consisting of a linear part \mathbf{K}_L :

$$(2.7) \quad \mathbf{K}_L = \sum_{i=1}^n (\mathbf{C}^e)^T \bar{K}_L^e \mathbf{C}^e, \quad \bar{K}_L^e = (\mathbf{T}^e)^T \mathbf{K}_L^e \mathbf{T}^e,$$

$$\mathbf{K}_L^e = \frac{E^e A^e}{L^e} \begin{bmatrix} \mathbf{I}_0 & -\mathbf{I}_0 \\ -\mathbf{I}_0 & \mathbf{I}_0 \end{bmatrix}, \quad \mathbf{I}_0 = \begin{bmatrix} 1 & 0 & 0 \\ 0 & 0 & 0 \\ 0 & 0 & 0 \end{bmatrix}$$

and a part including the initial prestress $S \mathbf{K}_G(\mathbf{S})$, where $\mathbf{S} = \mathbf{y}_S S$:

$$(2.8) \quad \mathbf{K}_G(\mathbf{S}) = \sum_{i=1}^n (\mathbf{C}^e)^T \mathbf{K}_G^e(S^e) \mathbf{C}^e,$$

$$\mathbf{K}_G^e(S^e) = \frac{S^e}{L^e} \begin{bmatrix} \mathbf{I} & -\mathbf{I} \\ -\mathbf{I} & \mathbf{I} \end{bmatrix}, \quad \mathbf{I} = \begin{bmatrix} 1 & 0 & 0 \\ 0 & 1 & 0 \\ 0 & 0 & 1 \end{bmatrix},$$

where: n – number of elements (e) in the structure, E^e – Young modulus, A^e – cross-sectional area, L^e – length, \mathbf{C}^e – Boolean matrix, \mathbf{T}^e – transformation matrix, S^e – initial prestress.

A detailed mathematical description of the discrete model can be found in [27].

After the determination of the coefficients, the polynomial expansions must be applied to all m degrees of freedom of the finite element model of the basic module:

$$(2.9) \quad \mathbf{q} = \mathbf{T}_1 \boldsymbol{\varepsilon},$$

where \mathbf{T}_1 ($\in \mathbb{R}^{m \times 60}$) – the first transformation matrix.

Substituting (2.9) into (2.5) the strain energy can be written as a function of the vector $\boldsymbol{\varepsilon}$:

$$(2.10) \quad E_s^{\text{FEM}} = \frac{1}{2} \boldsymbol{\varepsilon}^T \mathbf{T}_1^T \mathbf{K} \mathbf{T}_1 \boldsymbol{\varepsilon}.$$

Second transformation – elimination of linearly dependent displacements

A truss structure can perform as many linearly independent rigid body modes and deformation patterns as it has degrees of freedom. For example, an eight-degree-of freedom planar rectangle has 3 rigid body motions u, v, r 3 strains $\varepsilon_x, \varepsilon_y, \varepsilon_{xy}$ and 2 strain gradients $\varepsilon_{x,y}, \varepsilon_{y,x}$ (8 linearly independent variables) shown in Fig. 1. All linearly dependent variables and also rigid body motions must be eliminated for the next part of the analysis:

$$(2.11) \quad E_s^{\text{FEM}} = \frac{1}{2} \boldsymbol{\varepsilon}^T \mathbf{T}_2^T \mathbf{T}_1^T \mathbf{K} \mathbf{T}_1 \mathbf{T}_2 \boldsymbol{\varepsilon},$$

where $\mathbf{T}_2 (\in \mathbb{R}^{m \times i})$ – the second transformation matrix, i – the number of independent strains decreased by the number of rigid body motions.

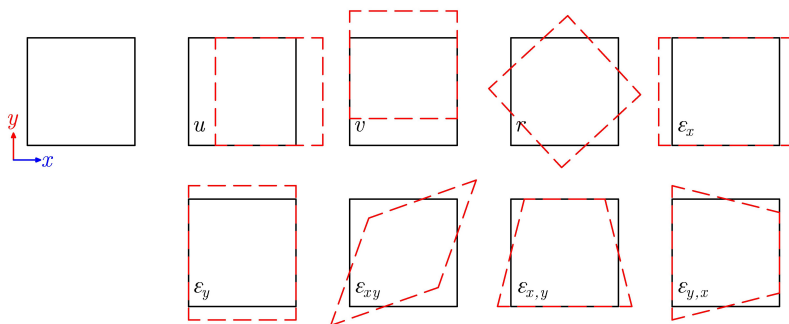


FIG. 1. Linearly independent configurations for an 8-degree of freedom planar structure.

The set of linearly independent coefficients can be determined by calculation of the rank of the \mathbf{T}_1 matrix [12] or the application of kinematic constraints [17].

Third transformation – fundamental strains first

In the third transformation, the strain vector $\boldsymbol{\varepsilon}$ is decomposed as:

$$(2.12) \quad \boldsymbol{\varepsilon} = \begin{bmatrix} \boldsymbol{\alpha} \\ \boldsymbol{\beta} \end{bmatrix},$$

where $\boldsymbol{\alpha} (\in \mathbb{R}^{5 \times 1})$ – the resultant fundamental strain; in the considered case $\boldsymbol{\alpha} = [\varepsilon_x \ \varepsilon_y \ \varepsilon_{xy} \ \varepsilon_{x,z} \ \varepsilon_{y,z}]^T$, $\boldsymbol{\beta} (\in \mathbb{R}^{(i-5) \times 1})$ – the rest of the coefficients.

The above modification yields:

$$(2.13) \quad E_s^{\text{FEM}} = \frac{1}{2} \begin{bmatrix} \boldsymbol{\alpha} \\ \boldsymbol{\beta} \end{bmatrix}^T \mathbf{T}_3^T \mathbf{T}_2^T \mathbf{T}_1^T \mathbf{K} \mathbf{T}_1 \mathbf{T}_2 \mathbf{T}_3 \begin{bmatrix} \boldsymbol{\alpha} \\ \boldsymbol{\beta} \end{bmatrix} = \frac{1}{2} \begin{bmatrix} \boldsymbol{\alpha} \\ \boldsymbol{\beta} \end{bmatrix}^T \mathbf{S} \begin{bmatrix} \boldsymbol{\alpha} \\ \boldsymbol{\beta} \end{bmatrix},$$

where $\mathbf{T}_3 \in \mathbb{R}^{m \times i}$ – the third transformation matrix.

This step can be easily omitted by putting the resultant fundamental strain $\boldsymbol{\alpha}$ on the first positions of the strain vector $\boldsymbol{\varepsilon}$ at the beginning of the analysis.

Fourth transformation – static condensation or omission of higher order strains

In the last transformation, the dimension of the matrix $\mathbf{S} \in \mathbb{R}^{i \times i}$ is further reduced to $\mathbf{E} \in \mathbb{R}^{5 \times 5}$. The matrix \mathbf{S} is decomposed into four submatrices: $\mathbf{K}_{11} \in \mathbb{R}^{5 \times 5}$, $\mathbf{K}_{12} \in \mathbb{R}^{5 \times (i-5)}$, $\mathbf{K}_{21} \in \mathbb{R}^{(i-5) \times 5}$ and $\mathbf{K}_{22} \in \mathbb{R}^{(i-5) \times (i-5)}$, so (2.13) takes the form:

$$(2.14) \quad E_s^{\text{FEM}} = \frac{1}{2} \begin{bmatrix} \boldsymbol{\alpha} \\ \boldsymbol{\beta} \end{bmatrix}^T \begin{bmatrix} \mathbf{K}_{11} & \mathbf{K}_{12} \\ \mathbf{K}_{21} & \mathbf{K}_{22} \end{bmatrix} \begin{bmatrix} \boldsymbol{\alpha} \\ \boldsymbol{\beta} \end{bmatrix} = \frac{1}{2} \boldsymbol{\alpha}^T \mathbf{E} \boldsymbol{\alpha}.$$

The fourth transformation can be performed by two methods. The first approach uses the static condensation technique, which preserves the possible deformation patterns coupled with the fundamental strains, and matrix \mathbf{E} takes a form:

$$(2.15) \quad \mathbf{E} = \mathbf{K}_{11} - \mathbf{K}_{12} \mathbf{K}_{22}^T \mathbf{K}_{21}.$$

The second, simpler approach, proposed in [14–16], is to omit the rows and columns associated with the vector $\boldsymbol{\beta}$ in (2.14), so matrix (2.15) is:

$$(2.16) \quad \mathbf{E} = \mathbf{K}_{11}.$$

2.2.2. Linear six-parameter shell theory. To obtain closed forms for maximum displacements of tensegrity grids, the six-parameter shell theory was used [18–24]. In the considerations, the shell theory is simplified, assuming that plates have no curvature and due to small translations and rotations of the orthotropic model, the theory is linear. This kinematic model is formally equivalent to the Cosserat continuum with six independent degrees of freedom: three translations and three rotations (with drilling degree of freedom). The application of the linear six-parameter shell theory to the analysis of plate-like orthotropic tensegrity structures was proposed, among others, in [16, 25, 26]. A rectangular plate of a constant thickness h in the Cartesian coordinate system (xyz) is considered (Fig. 2).

The behavior at any point of the considered reference middle surface $\Omega = \{(x, y) \in \Pi, z \in \langle -h/2; h/2 \rangle\}$ is defined by the generalized displacements \mathbf{q}^{2D} and the corresponding to them internal forces \mathbf{Q}^{2D} :

$$(2.17) \quad \begin{aligned} \mathbf{q}^{2D} &= \mathbf{q}(x, y) = [u \ v \ \psi \ \phi_x \ \phi_y \ w]^T, \\ \mathbf{Q}^{2D} &= \mathbf{Q}(x, y) = -[f_x \ f_y \ m_z \ m_x \ m_y \ f_z]^T. \end{aligned}$$

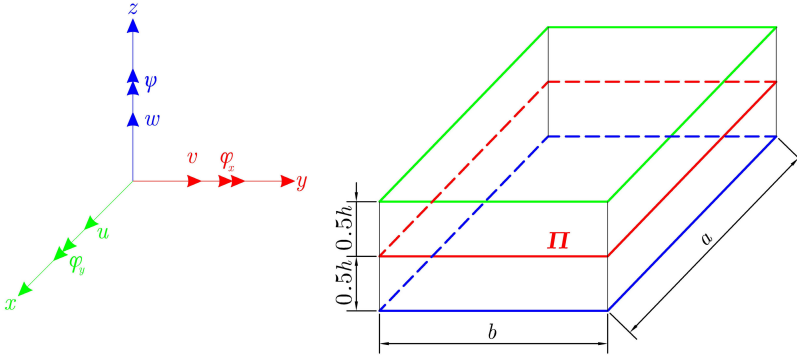


FIG. 2. Geometry of 3D plate-like body.

The first three displacements in (2.17) describe the membrane state, and the last three – the bending state. In general, these states are coupled, but if the middle surface is the reference plane of the plate model, they are not coupled. The equilibrium equations for the plate can be written as:

$$(2.18) \quad \mathbf{L}\mathbf{q}(x, y) = \mathbf{Q}(x, y),$$

where:

$$\mathbf{L} = h \begin{bmatrix} L_1 & L_4 & 0 & 0 & 0 & 0 \\ L_4 & L_2 & 0 & 0 & 0 & 0 \\ 0 & 0 & \alpha_2 \frac{h^2}{12} L_3 & 0 & 0 & 0 \\ 0 & 0 & 0 & \frac{h^2}{12} L_1 - \alpha_0 d_{55} & \frac{h^2}{12} L_4 & -\alpha_0 L_5 \\ 0 & 0 & 0 & \frac{h^2}{12} L_4 & \frac{h^2}{12} L_2 - \alpha_0 d_{44} & -\alpha_0 L_6 \\ 0 & 0 & 0 & \alpha_0 L_5 & \alpha_0 L_6 & \alpha_0 L_3 \end{bmatrix},$$

where:

$$\begin{aligned} L_1 &= d_{11} \frac{\partial^2}{\partial x^2} + d_{66} \frac{\partial^2}{\partial y^2}, & L_4 &= (d_{12} + d_{66}) \frac{\partial^2}{\partial x \partial y}, \\ L_2 &= d_{66} \frac{\partial^2}{\partial x^2} + d_{22} \frac{\partial^2}{\partial y^2}, & L_5 &= d_{55} \frac{\partial}{\partial x}, \\ L_3 &= d_{55} \frac{\partial^2}{\partial x^2} + d_{22} \frac{\partial^2}{\partial y^2}, & L_6 &= d_{44} \frac{\partial}{\partial y}. \end{aligned}$$

The behavior at any point of the considered plate strip or beam with the width a , is defined by generalized displacements \mathbf{q}^{1D} and the corresponding to them internal forces \mathbf{Q}^{1D} :

$$(2.19) \quad \begin{aligned} \mathbf{q}^{1D} &= \mathbf{q}(x) = [u \quad \psi \quad \phi_x w]^T, \\ \mathbf{Q}^{1D} &= \mathbf{Q}(x) = -a^2 [f_x \quad m_z \quad m_x f_z]^T. \end{aligned}$$

The equilibrium equations for plate strips or beams can be written as:

$$(2.20) \quad \tilde{\mathbf{L}}\mathbf{q}(x) = \mathbf{Q}(x),$$

where:

$$\tilde{L} = ha^2 \begin{bmatrix} d_{11} \frac{d^2}{dx^2} & 0 & 0 & 0 \\ 0 & \alpha_0 \frac{h^2}{12} d_{55} \frac{d^2}{dx^2} & 0 & 0 \\ 0 & 0 & \frac{h^2}{12} d_{11} \frac{d^2}{dx^2} - \alpha_0 d_{55} & -\alpha_0 d_{55} \frac{d}{dx} \\ 0 & 0 & \alpha_0 d_{55} \frac{d}{dx} & \alpha_0 d_{55} \frac{d^2}{dx^2} \end{bmatrix}.$$

By solving the system of differential equations (2.18) and (2.20), the explicit formulas of displacements and internal forces can be obtained for any load and support conditions.

In the paper, simply supported plate-like structures loaded with a uniformly distributed load p were considered and the load function was assumed as $f_z(xy) = -\frac{16p}{\pi^2} \sin \frac{\pi x}{a} \sin \frac{\pi y}{b}$. The maximum displacement was assumed as the first element of the Fourier series of the deflection function $w_{\text{plate}}(xy) = w_0 \sin \frac{\pi x}{a} \sin \frac{\pi y}{b}$. The following shear coefficients were assumed: $\alpha_0 = 5/6$, $\alpha_2 = 7/10$ [24–26].

Solving Eqs. (2.18), the formula for the maximum deflection of a plate-like structure was obtained:

$$(2.21) \quad w_{\text{plate,max}} = -\frac{16a^2b^2}{\alpha_0 h^3 \pi^6} \frac{A}{B} p,$$

where:

$$\begin{aligned} A &= 144\alpha_0^2 a^4 b^4 d_{44} d_{55} \\ &\quad + (12\alpha_0 a^2 b^2 [a^2(d_{22} d_{55} + d_{44} d_{66}) + b^2(d_{11} d_{44} + d_{55} d_{66})] h^2 \pi^2 \\ &\quad + [b^4 d_{11} d_{66} + a^4 d_{22} d_{66} - a^2 b^2 (d_{12}^2 - d_{11} d_{22} + 2d_{12} d_{66})] h^4 \pi^4), \\ B &= [12\alpha_0 a^2 b^2 d_{44} d_{55} (b^4 d_{11} + 2a^2 b^2 d_{22} (d_{12} + 2d_{66})) \\ &\quad + (a^2 d_{44} + b^2 d_{55}) [b^4 d_{11} d_{66} + a^4 d_{22} d_{66} \\ &\quad - a^2 b^2 (d_{12}^2 - d_{11} d_{22} + 2d_{12} d_{66})]] h^2 \pi^2. \end{aligned}$$

In turn, simply supported beam-like structures loaded with a uniformly distributed load p were considered and the load function was assumed as $f_z(x) = -p$. The maximum displacement was assumed as a polynomial function $w(x)$. Solving Eqs. (2.20), the formula for the maximum deflection of a beam-like structure was obtained:

$$(2.22) \quad w_{\text{beam,max}} = -\frac{a^2 p}{h} \left[\frac{5}{32} \left(\frac{a}{h} \right)^2 \frac{1}{d_{11}} + \frac{1}{8} \frac{1}{\alpha_0 d_{55}} \right].$$

2.2.3. Discrete model. To describe the behavior of double-layered tensegrity grids, a geometrically nonlinear model with large gradients of displacements but small strain gradients was adopted. Due to the specificity of tensegrity structures, the condition of initial prestress related to the introduction of the self-stress state was additionally taken into account. The total Lagrangian approach was adopted (Lagrange stationary description). The incremental static equilibrium equation of the structure takes the following form:

$$(2.23) \quad \mathbf{K}_T(\mathbf{q})\Delta\mathbf{q} = \Delta\mathbf{P} + \mathbf{R},$$

where: $\Delta\mathbf{q}$ ($\in \mathbb{R}^{m \times 1}$) – the vector of displacement increments, $\Delta\mathbf{P}$ ($\in \mathbb{R}^{m \times 1}$) – the vector of nodal forces increments, \mathbf{R} ($\in \mathbb{R}^{m \times 1}$) – the residual force vector, $\mathbf{K}_T(\mathbf{q})$ ($\in \mathbb{R}^{m \times m}$) – the tangent stiffness matrix of structure:

$$(2.24) \quad \mathbf{K}_T(\mathbf{q}) = [\mathbf{K}_L + \mathbf{K}_G(\mathbf{S}) + \mathbf{K}_{NL}(\mathbf{q})],$$

where $\mathbf{K}_{NL}(\mathbf{q})$ ($\in \mathbb{R}^{m \times m}$) – the nonlinear displacement stiffness matrix.

The residual force vector \mathbf{R} ($\in \mathbb{R}^{m \times 1}$) in (2.23) results from the aggregation. In equilibrium it is equal zero ($\mathbf{R} = 0$), while in the iteration process, the norm $\|\mathbf{R}\|$ is the “distance” from the equilibrium state. The iterative process converges if $\|\mathbf{R}\| \rightarrow 0$.

To solve the system of non-linear equations (2.23), numerical iterative or incremental-iterative techniques [29, 30, 32, 33] should be used. In this paper, the Newton–Raphson method [33] was applied.

3. Numerical applications

In the paper, the validation of proposed orthogonal continuum model was considered. To verify the procedure, a non-tensegrity plate-like structure was considered firstly. Next, the basic orthotropic tensegrity module was introduced. It was made of four modified Quadruplex modules clustered in the way that provides orthotropic properties of the structure. Due to the fact that the upper surface of the modified module is inscribed into the lower one, it was possible to easily combine individual units into multi-module structures. Then, beam-like and plate-like tensegrity structures built from the basic orthotropic module were considered. Particularly, the influence of the initial prestress S on stiffness and displacements was analyzed. In the analysis, it is necessary to specify the minimum and maximum prestress levels. The lowest level of initial prestress S_{\min} must ensure the appropriate identification of the element type (cables or struts), while maximum S_{\max} should not increase the loads above the limits of the load-bearing elements.

In continuum modeling, two different procedures should be distinguished: for structures without mechanisms and for structures with mechanisms. For the first case (no mechanisms), the matrix \mathbf{E} was obtained according to (2.16) (without static condensation) and the first order theory was applied. In turn, for structures with mechanisms, the matrix \mathbf{E} should be determined accordingly to (2.15) (a full procedure) and the second order theory should be adopted.

In discrete modeling (FEM), three theories were used [27]. For structure without mechanisms, a linear setting (the first order theory) was applied, while for structures with mechanisms, the quasi linear (the second order theory) and nonlinear approach (the third order theory) were assumed. The calculations were made using a program written in the Mathematica environment.

3.1. Non-tensegrity structure

In order to verify the correctness of the applied procedure, a simply supported plate-like structure was considered. The structure is built from sixty-four repeatable cubic units with the dimension a (Fig. 3). The repeatable unit (Fig. 3a) and thus the entire structure have orthotropic properties. The analyzed plate-like structure is not a tensegrity due to the lack of mechanisms and self-stress states $\mathbf{y}_S = \mathbf{0}$. For such a structure, the stiffness matrix (2.6) consists only of the linear

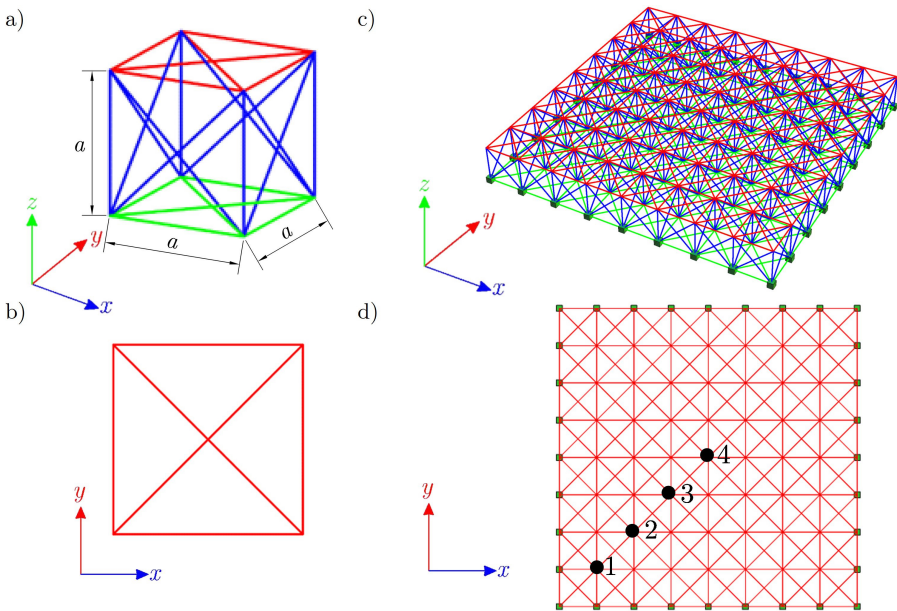


FIG. 3. Non-tensegrity structure: a) repeatable module – view 3D, b) repeatable module – top view, c) plate-like structure – view 3D, d) plate-like structure – top view.

part $\mathbf{K} = \mathbf{K}_L$. It is assumed that all elements are made of steel with Young's modulus E and of a profile with the cross sectional area A . The equivalent stiffness properties were obtained by omitting the terms related to strain gradients (2.16) and are as follows:

$$(3.1) \quad \mathbf{E} = \frac{EA}{a} \begin{bmatrix} 6.83 & 1.41 & 0 & 0 & 0 \\ & 6.83 & 0 & 0 & 0 \\ & & 6.83 & 0 & 0 \\ & & & 5.65 & 0 \\ sym. & & & & 5.65 \end{bmatrix}.$$

The discrete model consists of nine hundred and thirteen elements ($n = 913$), one hundred and sixty-two nodes ($w = 162$) and three hundred and ninety degrees of freedom ($m = 390$). The structure is simply supported on four edges. Due to the lack of mechanisms, the first order theory was applied.

TABLE 1. Comparison of the maximum displacement for the non-tensegrity plate-like structure.

No. of point (Fig. 3d)	Displacement [a/EA]		Error [%]
	discrete model	continuum model	
1	34 440	32 261.2	6.71
2	103 530	110 147	-6.29
3	168 000	188 032	-11.88
4	193 410	220 293	-13.90

The displacements of structures were calculated taking into account a uniformly distributed load $p = -5 \text{ kN/m}^2$ applied on the upper surface of the structure. The comparison of the displacements obtained according to the discrete model and the continuum model is shown in Table 1. Comparing the numerical results, it can be seen that the method gives the results with sufficient accuracy. The biggest relative error was obtained for the maximum displacement (point 4 – Fig. 3d). In turn, comparing the shape of the deformed structure (Fig. 4), it can be observed that the assumed Fourier series as the deflection function $w(xy) = w_0 \sin \frac{\pi x}{a} \sin \frac{\pi y}{b}$ does not describe the structure accurately.

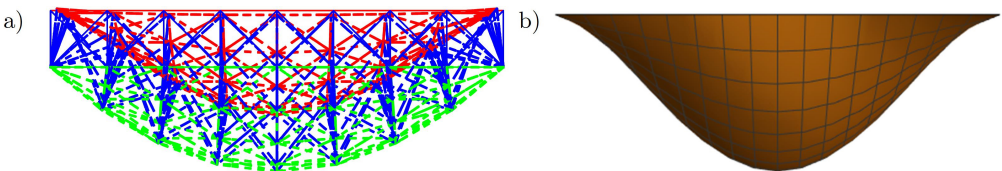


FIG. 4. Shape of the deformed structure: a) discrete model, b) continuum model.

3.2. Basic orthotropic four-module tensegrity grid

The main aim of the paper was to use the continuum orthotropic model to build tensegrity grids. An unsupported basic module built from modified Quadruplex modules was proposed. The single modified Quadruplex module consists of 4 struts, 12 cables and has dimensions allowing it to fit into a unit cube, i.e. $a=1$. Four single modules (Fig. 5) are joined axisymmetrically to achieve orthotropic properties. The analyzed basic module is a tensegrity structure characterized by 7 mechanism (6 finite and one infinitesimal) and 4 self-stress states. In the quantitative analysis, the self-stress state \mathbf{y}_S for the single modified Quadruplex module [27] was taken into account. A self-equilibrated system of normal forces \mathbf{S} in a function of the initial prestress S was specified ($\mathbf{S} = \mathbf{y}_S S$). It is assumed that all elements are made of steel with Young's modulus E and of a profile with cross sectional area respectively A_c for cables and A_s for struts. The equivalent stiffness properties were obtained firstly by omitting the terms related to strain gradients (2.16) and secondly by static condensation (2.15). In the first, a simplified approach, it was possible to obtain closed forms of the equivalent stiffness properties:

$$\begin{aligned}
 (3.2) \quad d_{11} &= d_{22} = (9.10EA_c + 2.52EA_z)/a, \\
 d_{12} &= (2.83EA_c + 1.19EA_z)/a, \\
 d_{44} &= (11.31EA_c + 4.74EA_z)/a, \\
 d_{55} &= d_{66} = (4.29EA_c + 11.85EA_z)/a.
 \end{aligned}$$

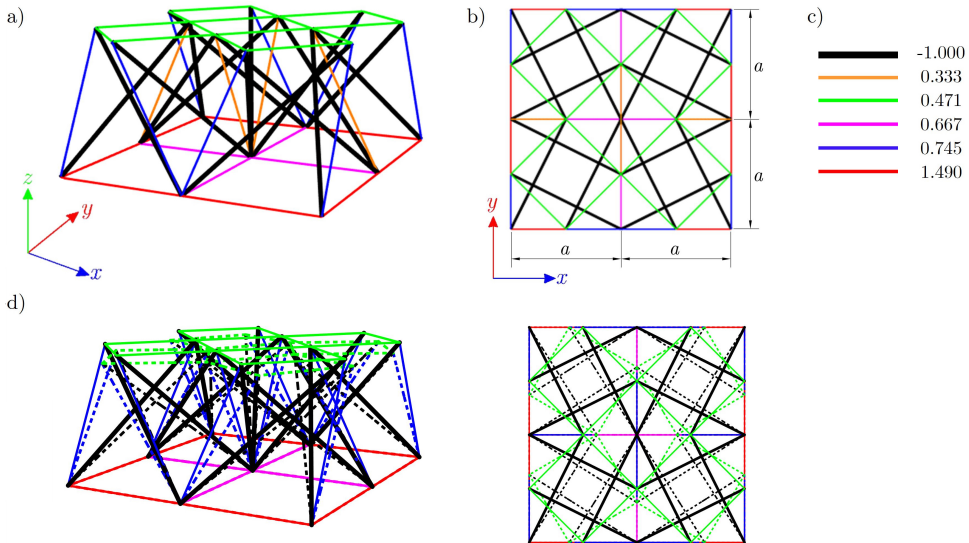


FIG. 5. Base orthotropic model: a) view 3D, b) top view, c) self-stress forces, d) shape of the mechanism.

Analyzing the formulas (3.2), it can be observed that the coefficients of matrix \mathbf{E} do not depend on the level of initial prestress S . In the second approach (a full procedure), it was impossible to obtain results in closed forms and only numerical values can be obtained.

It is assumed that the cables (marked in red, magenta, orange, green or blue lines respectively to the self-stress force) are made of steel S460N. The type A cables with Young’s modulus $E = 210 \text{ GPa}$ [33] are used. The struts (marked in black lines) are made of hot-finished circular hollow section (steel S355J2) with Young’s modulus $E = 210 \text{ GPa}$. The density of steel is $\rho = 7860 \text{ kg/m}^3$. As cables, rods with diameter $\varphi = 20 \text{ mm}$ and the cross sectional area $A_c = 3.14 \text{ cm}^2$ are assumed, whereas as struts – pipes with diameter $\varphi = 76.1 \text{ mm}$, thickness $t = 2.9 \text{ mm}$ and the cross sectional area $A_z = 6.88 \text{ cm}^2$. The maximum prestress level is assumed as $S_{\max} = 60 \text{ kN}$ (the maximum effort of the structure is equal 0.83). For such data, the equivalent stiffness properties obtained without static condensation (3.2) are equal:

$$(3.3) \quad \begin{aligned} d_{11} = d_{22} &= 964019 \text{ kN/m}, & d_{12} &= 357836 \text{ kN/m}, \\ d_{44} &= 1431350 \text{ kN/m}, & d_{55} = d_{66} &= 1995600 \text{ kN/m}, \end{aligned}$$

while those obtained with using static condensation (a full procedure) are showed in Fig. 6.

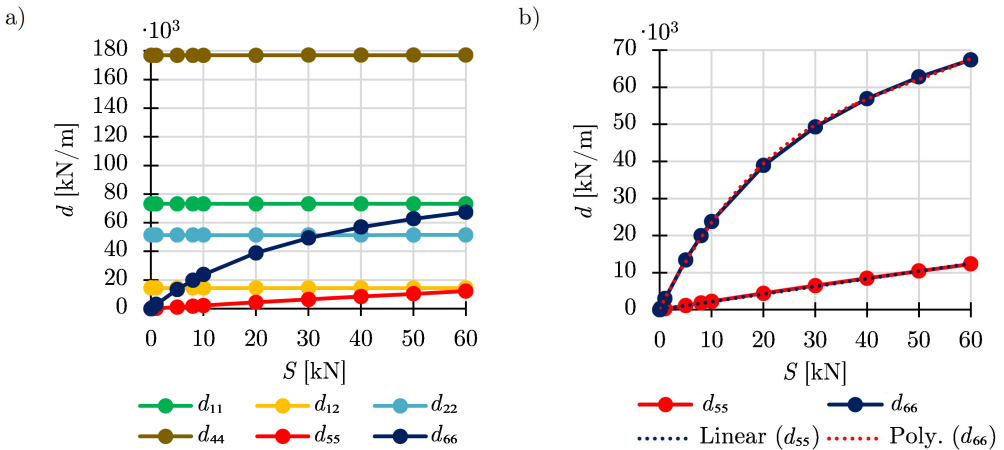


FIG. 6. Influence of the initial prestress S on the equivalent stiffness properties obtained using full procedure: a) all coefficients, b) coefficients depending on the initial prestress S (dotted lines – trend lines).

Four out of six equivalent stiffness properties, i.e. d_{11}, d_{12}, d_{22} and d_{44} , obtained using the full procedure, practically do not depend on the level of the initial prestress S (Fig. 6a). For example, the coefficient d_{11} equal respectively

$d_{11} = 73201.1$ kN for $S = 0$ and $d_{11} = 73228.8$ kN for S_{\max} – the difference is 0.04%. The average values of these coefficients are:

$$(3.4) \quad \begin{aligned} d_{11} &= 73211.5 \text{ kN/m}, & d_{12} &= 14390.9 \text{ kN/m}, \\ d_{22} &= 51377.7 \text{ kN/m}, & d_{44} &= 176924.9 \text{ kN/m}. \end{aligned}$$

Only two of them, i.e. d_{55} and d_{66} , depend on the level of initial prestress S . It is due to the shape of the mechanism, similarly like in [12, 13]. The coefficient d_{55} equal respectively $d_{55} = 0$ kN for $S = 0$ and $d_{11} = 12306.1$ kN for S_{\max} , whereas d_{66} varies from to 67408.7 kN. The obtained numerical results allowed determining trend lines (Fig. 6b):

$$(3.5) \quad \begin{aligned} d_{55} &= 206.82S + 108.8 \text{ [kN/m]}, \\ d_{66} &= 0.3114S^3 - 45.629S^2 + 2739.7S + 330.56 \text{ [kN/m]} \end{aligned}$$

with coefficients of determination $R^2 = 0.9992$ for d_{55} and $R^2 = 0.9997$ for d_{66} , respectively.

3.3. Tensegrity structures

The obtained basic orthotropic module was used to build a simply supported tensegrity beam-like (Fig. 7) and a plate-like structure (Fig. 8). The first structure is built from 4 basic modules, whereas the second one – from 16 basic modules. Both structures are characterized by one mechanism. For such structures, the second order theory was assumed and the stiffness matrix (2.6) is used. For comparison, a matrix \mathbf{E} was obtained according to (2.16) (without static condensation) and according to (2.13) (a full procedure). The discrete model of beam-like structure consists of two hundred and twelve elements ($n = 212$), sixty nine nodes ($w = 69$) and one hundred and fifty-nine degrees of freedom ($m = 159$). The structure is simply supported on two shorter edges. In turn, the

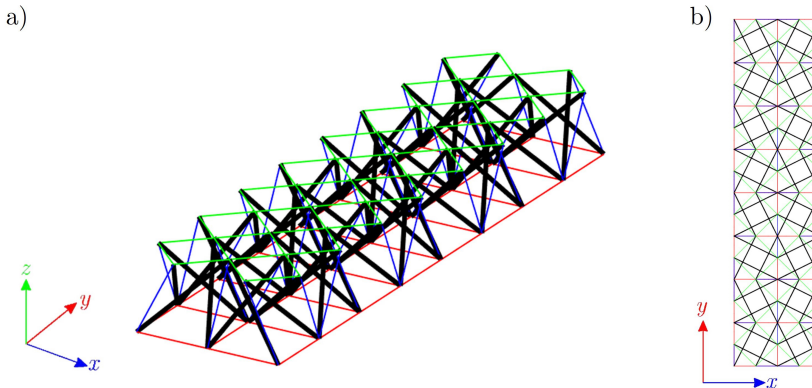


FIG. 7. Beam-like structure: a) view 3D, b) top view.

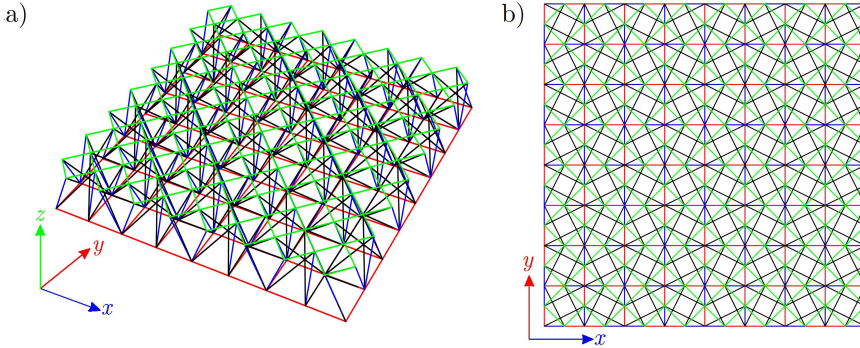


FIG. 8. Plate-like structure: a) view 3D, b) top view.

plate-like structure consists of eight hundred elements ($n = 800$), two hundred and twenty five nodes ($w = 225$) and five hundred and seventy-nine degrees of freedom ($m = 579$). The structure is simply supported on four edges. In both cases, the second order theory and the third order theory were applied. Both structures were loaded with a uniformly distributed load $p = -1.5 \text{ kN/m}^2$ applied on the upper surface of the structure.

The comparison of the results obtained for the beam-like structure from continuum modeling and discrete modeling is presented in Fig. 9a, while for the

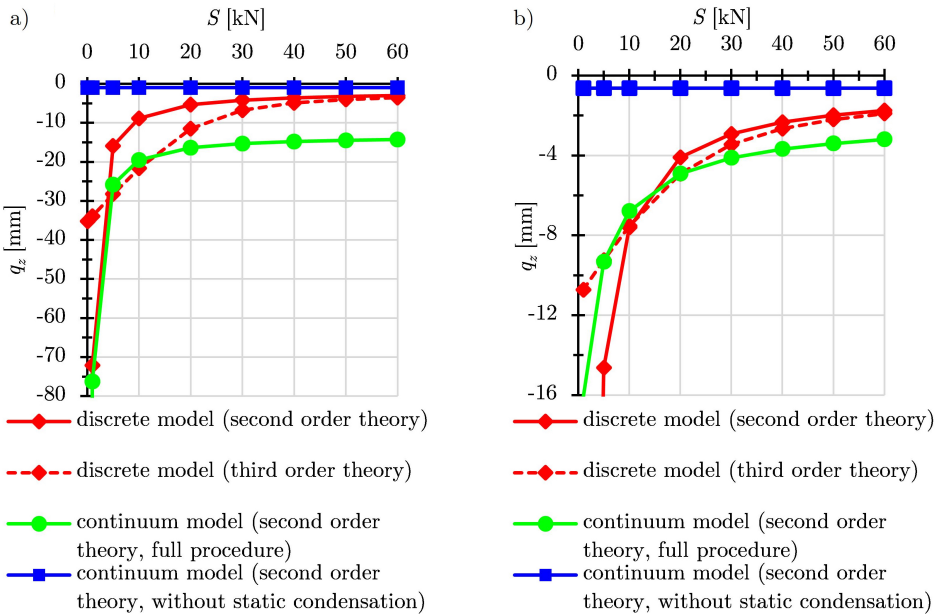


FIG. 9. Comparison of the maximum displacement for the: a) beam-like structure, b) plate-like structure.

plate-like structure – in Fig. 9b. Since the continuum model was derived from the matrices of the quasi-linear theory (the second order theory), the results should be compared with the respective discrete model (a red continuous line). Continuum modeling without static condensation (a blue line) gives inappropriate results because of the fact that equivalent continuum stiffness coefficients do not depend on the level of the prestress level. The static condensation utilized in this paper provides more accurate results and gives a better approximation (a green line). For plate-like structures, the deflection function is not exact (as shown in the example of the non-tensegrity structure), but for the beam-like structure, using a polynomial function as a deflection function gives a better fit.

The differences between the discrete and proposed continuum model were caused by the use of the second order theory. This approach does not take into account stiffening of the structure under the influence of an external load. Further considerations should also take into account nonlinearity (the third order theory, marked with a red dashed line), that gives an exact result for tensegrity structures. The inaccuracy of results can also be caused by the application of conventional shear coefficient factors. Their values should be verified.

4. Conclusions

The article fills the gap in the existing literature and is the first attempt to validate the global behavior of beam- and plate-like tensegrity structures modeled using the continuum approach and characterized by the existence of mechanisms. The full analysis is a two-step process. The first step involves developing a continuum model and the second is validating the model. Unlike conventional truss systems, in the case of tensegrity structures, the proposed approach must take into account the level of the prestress level. This work took into account the effective properties of a single repeating unit (i.e. a tensegrity module). These units were used to build the tensegrity beam- or plate-like structures.

For the development of the continuum model, a procedure called the energy equivalence method was adopted. The basis of this approach is the assumption that the finite element strain energy of a deformed tensegrity truss system contains the same energy as its continuum counterpart. To take advantage of the equality of energy, the nodal displacements of the discrete model must be represented in terms of the strains of the continuum. A single repeating orthotropic unit was isolated from the whole structure. It was assumed that the displacement field of this unit was described by the third-order polynomials and expanded into the Taylor series. The above procedure led to the determination of the transformation matrix which enables obtaining the effective stiffness properties of the continuum model. The application of the second order theory allowed obtain-

ing explicit formulas of the stiffness matrix for the repeating orthotropic unit. The quasi-linear approach was a simplification, but it was sufficient to verify the applicability of continuum modeling and assesses the possibility of its future development.

The second step was to validate the obtained continuum model. This process completed the analysis and is vital for the practical application. The validation consisted in comparing the displacements obtained for the continuous and discrete models. The numerical analysis was provided by the calculation procedure written in the Mathematica environment.

The presented results were the first attempt to verify continuum modeling of tensegrity beam- and plate-like structures characterized by mechanisms. The previous research validated only the coefficients of the stiffness matrix of the continuum model, not the global behavior of tensegrity structures. The obtained results gave satisfying accuracy, but they can be further improved. To fully explore the potential of continuum modeling, more examples need to be provided to draw a more general conclusion. As shown in the example of a non-tensegrity structure, the deformed shape of a structure modeled discretely was different than of a structure modeled as continuum. For plate-like structures, a better fit of the shape function could be achieved with a polynomial function instead of a Fourier series. When deriving a continuum model, the third order theory stiffness matrix should be introduced. In the work, only second order theory matrices were taken into account for the continuum modeling. This is not a sufficient approach and was used due to its simplicity in order to validate the applicability of the proposed continuum model. Another aspect that may affect the results is the need to verify the application of conventional shear factors in the six-parameter theory. As the behavior of tensegrities is significantly affected by the existence of the self-stress state, the coefficient should probably vary with the change of the prestress level.

References

1. Y. KONO, K.K. CHOONG, T. SHIMADA, H. KUNIEDA, *An experimental investigation of a type of double-layer tensegrity grids*, Journal of the International Association for Shell and Spatial Structures, **40**, 2, 103–111, 1999.
2. W. GILEWSKI, J. KŁOSOWSKA, P. OBARA, *Verification of tensegrity properties of kono structure and blur building*, XXV Polish – Russian – Slovak Seminar “Theoretical Foundation of Civil Engineering”, **153**, 173–179, 2016.
3. L. CRAWFORD, *Transgender Architectonics: the Shape of Change in Modernist Space*, Routledge, 2015.
4. V. GOMEZ-JAUREGUI, R. ARIAS, C. OTERO, C. MANCHADO, *Novel technique for obtaining double-layer tensegrity grids*, International Journal of Space Structures, **27**, 155–166, 2012.

5. B.-B. WANG, *Cable-strut systems: part I – tensegrity*, Journal of Constructional Steel Research, **45**, 3, 281–289, 1998.
6. P. OBARA, J. TOMASIK, *Parametric analysis of tensegrity plate-like structures: part 2 – quantitative analysis*, Applied Sciences, **11**, 2, 2021.
7. M. LIU, D. CAO, J. WEI, *Survey on equivalent continuum modeling for truss structures and their nonlinear dynamics and vibration control*, Journal of Vibration Engineering & Technologies, **10**, 2, 667–687, 2022.
8. A.K. NOOR, M.M. MIKULAS, *Continuum Modeling of Large Lattice Structures: Status and Projections*, NASA Technical Paper 2767, 1988.
9. A.K. NOOR, *Continuum modeling for repetitive lattice structures*, Applied Mechanics Reviews, **41**, 7, 285–296, 1988.
10. A. TEUGHEL, G. DE ROECK, *Continuum models for beam- and platelike lattice structures*, IASS-IACM 2000, 4th International Colloquium on Computation of Shell and Spatial Structures, 2000.
11. M.P. NEMETH, *A Treatise on Equivalent-Plate Stiffnesses for Stiffened Laminated-Composite Plates and Plate-Like Lattices*, NASA Technical Paper 2011-216882, 2011.
12. K. KEBICHE, M.N.K. AOUAL, R. MOTRO, *Continuum Models for Systems in a Selfstress State*, International Journal of Space Structures, **23**, 2, 103–115, 2008.
13. K. YILDIZ, G.A. LESIEUTRE, *Effective Beam Stiffness Properties of n-Strut Cylindrical Tensegrity Towers*, AIAA Journal, **57**, 5, 2185–2194, 2019.
14. A. AL SABOUNI-ZAWADZKA, W. GILEWSKI, *On Orthotropic Properties of Tensegrity Structures*, XXV Polish–Russian–Slovak Seminar Theoretical Foundation of Civil Engineering, **153**, 887–894, 2016.
15. A. AL SABOUNI-ZAWADZKA, W. GILEWSKI, *Technical Coefficients in Continuum Models of an Anisotropic Tensegrity Module*, Procedia Engineering, **111**, 871–876, 2015.
16. A. AL SABOUNI-ZAWADZKA, J. KŁOSOWSKA, P. OBARA, W. GILEWSKI, *Continuum model of orthotropic tensegrity Plate-Like structures with Self-Stress included*, Engineering Transactions, **64**, 501–508, 2016.
17. J.O. DOW, Z.W. SU, C.C. FENG, C. BODLEY, *Equivalent continuum representation of structures composed of repeated elements*, AIAA Journal, **23**, 10, 1564–1569, 1985.
18. A. LIBAI, J.G. SIMMONDS [eds.], *The Nonlinear Theory of Elastic Shells. One Spatial Dimension*, Academic Press, 1988.
19. J. CHRÓŚCIELEWSKI, J. MAKOWSKI, W. PIETRASZKIEWICZ, *Statics and Dynamics of Multifold Shell: Nonlinear Theory and Finite Element Method*, IPPT PAN, Warsaw, 2004 [in Polish].
20. S. BURZYŃSKI, J. CHRÓŚCIELEWSKI, K. DASZKIEWICZ, W. WITKOWSKI, *Geometrically nonlinear FEM analysis of FGM shells based on neutral physical surface approach in 6-parameter shell theory*, Composites Part B: Engineering, **107**, 203–213, 2016.
21. J. CHRÓŚCIELEWSKI, I. KREJA, A. SABIK, W. WITKOWSKI, *Modeling of composite shells in 6-parameter nonlinear theory with drilling degree of freedom*, Mechanics of Advanced Materials and Structures, **18**, 6, 403–419, 2011.

22. S. BURZYŃSKI, J. CHRÓSCIELEWSKI, W. WITKOWSKI, *Geometrically nonlinear FEM analysis of 6-parameter resultant shell theory based on 2-D Cosserat constitutive model*, ZAMM – Journal of Applied Mathematics and Mechanics / Zeitschrift für Angewandte Mathematik und Mechanik, **96**, 2, 191–204, 2016.
23. W. PIETRASZKIEWICZ, *The resultant linear six-field theory of elastic shells: what it brings to the classical linear shell models?*, ZAMM – Journal of Applied Mathematics and Mechanics / Zeitschrift für Angewandte Mathematik und Mechanik, **96**, 8, 899–915, 2016.
24. W. WITKOWSKI, *Synthesis of Formulation of Nonlinear Mechanics of Shells Undergoing Finite Rotations in The Context of FEM*, Gdańsk University of Technology Publishing House, Gdańsk, 2011.
25. P. OBARA, *Application of linear six-parameter shell theory to the analysis of orthotropic tensegrity plate-like structures*, Journal of Theoretical and Applied Mechanics, **57**, 167–178, 2019.
26. P. OBARA, *Analysis of orthotropic tensegrity plate strips using a continuum two-dimensional model*, MATEC Web Conference, **262**, 2019.
27. W. GILEWSKI, J. KŁOSOWSKA, P. OBARA, *Application of singular value decomposition for qualitative analysis of truss and tensegrity structures*, Acta Scientiarum Polonorum Hortorum Cultus, **14**, 3, 14, 2015.
28. P. OBARA, J. TOMASIK, *Parametric Analysis of tensegrity plate-like structures: part 1 – qualitative analysis*, Applied Sciences, **10**, 20, 2020.
29. K.-J. BATHE, *Finite Element Procedures in Engineering Analysis*, Prentice-Hall, New Jersey, 1982.
30. O.C. ZIENKIEWICZ, R.L. TAYLOR, J.Z. ZHU (ed.), *The Finite Element Method: Its Basis and Fundamentals*, Butterworth-Heinemann, Oxford, 2013.
31. P. CHADWICK, M. VIANELLO, S.C. COWIN, *A new proof that the number of linear elastic symmetries is eight*, The Jean-Paul Boehler Memorial Volume, **49**, 11, 2471–2492, 2001.
32. J. SZMELTER, *Computer Methods in Mechanics*, Państwowe Wydawnictwo Naukowe, Warsaw, 1980 [in Polish].
33. G. RAKOWSKI, Z. KACPRZYK, *Finite Element Method in Structural Mechanics*, Warsaw University of Technology Publishing House, Warsaw, 2016 [in Polish].
34. EN 1993-1-11: 2006. Eurocode 3: Design of steel structures – Part 1-11: Design of structures with tension components.

Received November 19, 2022; revised version March 06, 2023.

Published online April 20, 2023.
